Journal of The
Electrochemical Society

Understanding Redox Organic Behavior in Deep Eutectic Solvents: Considerations for Molecular Design

To cite this article before publication: Nicholas S Sinclair *et al* 2025 *J. Electrochem. Soc.* in press https://doi.org/10.1149/1945-7111/adb186

Understanding Redox Organic Behavior in Deep Eutectic Solvents: Considerations for Molecular Design

Journal:	*Journal of The Electrochemical Society*
Manuscript ID	JES-113524.R1
Manuscript Type:	Research Paper
Date Submitted by the Author:	21-Jan-2025

Complete List of Authors:	Sinclair, Nicholas; Case Western Reserve University, Chemical Engineering Abranches, Dinis; University of Aveiro Chemistry Department Savinell, Robert; Case Western Reserve University, Chemical Engineering Maginn, Edward; University of Notre Dame Department of Chemical and Biomolecular Engineering Wainright, Jess; Case Western Reserve University, Chemical Engineering

Keywords:	Deep Eutectic Solvents, Energy Storage, Batteries, flow battery

Understanding Redox Organic Behavior in Deep Eutectic Solvents- Considerations for Molecular Design

Nicholas S. Sinclair,[1,z] Dinis O. Abranches,[2,3] Robert F. Savinell,[1,**] Edward J. Maginn,[2] Jesse S. Wainright[1,*]

[1] Department of Chemical and Biomolecular Engineering, Case Western Reserve University, Cleveland, Ohio 44106, USA

[2] Department of Chemical and Biomolecular Engineering, University of Notre Dame, Notre Dame, Indiana 46556, USA

[3] CICECO – Aveiro Institute of Materials, Department of Chemistry, University of Aveiro, 3810-193 Aveiro, Portugal

*Electrochemical Society Member.

**Electrochemical Society Fellow.

[z]E-mail: nss20@case.edu

Abstract

Electrolytes based on deep eutectic solvents (DESs) coupled with redox active organic molecules have shown potential as a versatile and energy dense electrochemical energy storage system. However, progress in these systems has been held back by a lack of understanding of the irregular behavior displayed when redox active organic molecules are transitioned from other solvent systems. In this work, the hydrogen bonding characteristics of a series of redox organic molecules were investigated through infrared spectroscopy and molecular modeling. New understanding of these interactions was then used to explain their electrochemical behavior in a DES electrolyte. A model was used to predict the behavior of new derivatives towards the design of an optimized redox organic-DES system. Hydrogen bonding between the redox molecules and the solvent was found to significantly shift the potential of a redox reaction more positive when a hydrogen bond forms at the redox active site. It was predicted that functionalizing a molecule with electron withdrawing groups to lower the electron density of the redox active functional group lowers the strength of the hydrogen bond and thus alleviates the undesirable potential shift. This hypothesis was demonstrated by the addition of nitro groups to fluorenones.

Introduction

The demand for low cost, high performance energy storage has grown rapidly to complement the growing penetration of intermittent renewable energy generation and other grid related applications.[1–3] Electrochemical energy storage in the form of redox flow batteries can meet this demand due to their potential for low cost, safety, and flexibility, provided an optimal electrolyte and redox chemistry system can be developed.[4–7] Aqueous systems have energy density limitations due to the relatively small stable electrochemical window of water, making non-aqueous electrolyte systems of interest. Their larger potential window can allow for more extreme potential redox couples and thus higher energy densities without sacrificing safety or performance.[8,9] An appropriate set of redox couples is also required for a flow battery to function. Deep eutectic solvents (DESs) coupled with redox active organic molecules provide opportunities for molecular design to tune both the redox organic structure and the accompanying DES components in concert to enhance electrochemical, physical and transport characteristics and enable the electrolyte system to outperform existing technologies.[10,11]

DESs are a class of non-aqueous solvents prepared by physically mixing hydrogen bond donors (HBDs) and acceptors (HBAs).[12,13] They have recently gained interest because their physicochemical properties can be easily tuned by selecting different HBD/HBA combinations and mole ratios. DESs are interesting solvents for electrochemical applications,[14–16] because they are more stable at more extreme potentials than water with conductivities on the order of 10s of mS./cm, similar to other non-aqueous solvents.[17,18] In addition, they can be cheaper than other non-aqueous solvents such as acetonitrile, and safer due to their low vapor pressure. Their low vapor pressure allows them to be operated at elevated temperatures leading to higher conductivity and lower viscosity. [19,20] With redox organic-DES systems being a relatively unexplored concept, a greater understanding of these systems is necessary to develop these electrolytes into high performance energy storage systems. Given the electrochemically-favorable properties highlighted above, an appropriately designed redox organic DES can make a meaningful impact in electrochemical energy storage.[21–23]

To design redox organic-DES systems, we must understand how the redox active component interacts with the hydrogen bonding environment.[16,17,21,24] With a redox organic molecule, the interaction with the solvent can be complicated depending on the functional groups involved in the hydrogen bond interactions, and high solubilities (> 4M) can result. For example, methyl viologen, a commonly studied redox organic, has been utilized as an HBA in an ethylene glycol-based DES at concentrations up to 4.2 M. This is of interest for an energy storage system where the energy density is partially dictated by the concentrations of the two redox active components.[24]

Often redox organic molecules start as neutral molecules or stable radicals that are either oxidized to a cation or reduced to an anion. The nitroxide radical redox organic molecule known as PTIO (2-phenyl-4,4,5,5-tetrame- thylimidazoline-1-oxyl-3-oxide) is an example of a molecule that can be either oxidized to the cation or reduced to the anion. As such, it can provide both the positive and negative couples for a battery. Other redox active compounds such as methyl viologen are synthesized as cations, are dissolved into the electrolyte as salts, and are exclusively reduced and therefore used as negative couples. The potential at which these reactions occur for a given redox couple will be ideally as far apart as possible to maximize energy density and thus careful consideration is placed on the potential at which they can be oxidized or reduced when designing an electrolyte system.

The neutral (or radical) to cation reactions seen with TEMPO, the viologen derivatives, and the oxidation of PTIO appear reversible in DESs, but even if stable and soluble only comprise one half of the battery. Neutral (or radical) to anion couples in DESs often exhibit either irreversible behavior and/or extreme shifts in their apparent thermodynamic potential.[25,26] Often this behavior manifests as an extreme potential shift in only one of the redox peaks when compared to their electrochemical behavior in acetonitrile. Understanding these changes in behavior as a function the molecular structure of the various types of redox organic molecules is critical to the design of high energy density electrolytes for energy storage.

While surface adsorption may be the cause of some anomalous behavior as common DES components are known to surface adsorb to both carbon and platinum electrode surfaces,[27] it is also possible that new hydrogen bonds are being formed in DESs as the oxidation state of the redox organic molecules is changed. It has been reported that the strength of a hydrogen bond can be correlated to the electron density at a hydrogen bond critical point, i.e., the outermost section of the molecule where a hydrogen bond is formed. Hydrogen bonds of differing strengths can have drastically different physical properties.[28–32] This correlation has been modeled using *ab initio* methods and could be used to predict changes in the nature of a molecule's hydrogen bond interaction as it is functionalized and electron density near any redox functional group's changes.

In this work, various redox molecules were investigated that exhibit a variety of different behaviors in an acetonitrile electrolyte in comparison to a DES electrolyte. Voltammetry and infrared spectroscopy were performed on acetonitrile systems with and without the presence of ethylene glycol to determine the presence of hydrogen bonding, which functional groups are participating in hydrogen bonding, and if these effects can be correlated to changes in electrochemical behavior. High and low surface area electrodes were used to parse surface effects from bulk solution effects. Molecular modeling was then used to predict hydrogen bond strengths and positions to correlate to the known effects on electrochemical behavior. The creation of a predictive model based on these results was proposed to guide the design of redox organic molecules to maximize their effectiveness in a redox organic-DES energy storage electrolyte.

Experimental and Computational Methods

Voltammetry was performed in a dry nitrogen glove box with an approximate dew point of -75 °C. Choline chloride (ChCl, 99%), ethylene glycol (EG, Certified), sodium perchlorate ($NaClO_4$), ethyl viologen, PTIO, N-methylphthalimide, fluorenone, 2,7 di-nitro fluorenone and acetonitrile (HPLC) were all purchased from Fisher Scientific. Due to its deliquescent character, choline chloride was dried in a vacuum oven overnight at 90°C. EG was dried by stirring at 80 °C in a dry glove box. All other chemicals were used as received. A 1:4 molar ratio mixture of ChCl:EG, from here on referred to as the DES, was formulated in the dry box by heating the mixed components to 80 °C for 2 hours.[33] This molar ratio was chosen for its increased conductivity, reduced viscosity, and increased solubility of certain redox organic molecules as compared to the more commonly studied 1:2 molar ratio known as ethaline.[34] The DES solutions were then further dried by allowing them to equilibrate with the nitrogen dry box atmosphere while being stirred and heated to 50°C overnight. The water content of the prepared DES solution was measured using a Metrohm Coulometric KF 899 D and found to be less than 200 ppm.

Voltammetry was performed on a 1.6 mm diameter platinum disk working electrode, or a 3 mm glassy carbon disk as noted. All voltammetry was performed at room temperature (20 C +/- 2 C) for >10 cycles and are a representative steady state voltammetry after several cycles unless otherwise noted to display transient effects. Electrodes were purchased from BASi. A platinum mesh counter electrode was used. An in-house reference electrode was used, consisting of a platinum wire immersed in 10 mM silver nitrate when working in acetonitrile or a chloridized silver wire immersed in neat DES inside a fritted glass tube when working with DES. All electrochemical experiments were performed on a Solartron 1280B potentiostat.

Flow cell electrolysis was performed using an in-house 2.5 cm^2 flow cell design. The cell uses a flow through carbon felt configuration.[35] Impervious graphite current collectors were purchased from Graphite Store and machined in house. Morgan Advanced Materials WDF 3 mm thick graphite felt compressed to 2.5 mm was used as the high surface area electrode material. The graphite felt electrodes were heat treated at 400 °C for 4 hours prior to use. Daramic 175 (200 μm wetted thickness) was used as a porous separator. The Daramic was soaked in 2-propanol for 10 minutes to remove residual oil resulting from the manufacturing process, and then dried in air prior to use. All cells were operated at flow rates in excess of 20 times the stoichiometric minimum to minimize mass transport overpotentials.

Fourier transform infrared spectroscopy attenuated total reflectance (FTIR-ATR) samples were transferred from the glove box in sealed sample vials, but measurements were performed in ambient air conditions. ATR measurements were performed using a Nicolet iS50 FT-IR (Thermo Scientific, USA) with a diamond crystal. Thirty-two scans were collected per measurement. Background subtractions were performed using Omnic 9 software, version 9.8.372 (Thermo Scientific, USA).

Finally, all quantum chemistry calculations reported in this work were performed using the open-source, freely available software package NWChem (V6.8).[36,37] The geometry of each monomer (acetonitrile, EG, and the redox molecules at each oxidation state) was optimized in a double-stage fashion, with an initial run using Hartree-Fock (HF) and the def2-SVP basis set, followed by a DFT run with the B3LYP functional[38], the Grimme DFT-D3 dispersion correction[39], and the def2-TZVPD basis set. Three-dimensional electronic densities and electrostatic potentials were calculated using a resolution of 20 pm. Dimer geometries (EG or acetonitrile interacting with each redox active molecule) were also optimized using the aforementioned procedure and interaction energies (E) were calculated as the difference between the DFT energy of the dimer (E_{Dimer}) and that of each monomer (E_{M1} and E_{M2}), according to:

$$E = E_{Dimer} - (E_{M1} + E_{M2}) \quad (1)$$

Results and Discussion

Electrochemical Behavior: Acetonitrile vs DES Comparison

To determine redox activity and approximate reaction potentials, cyclic voltammetry, in which we sweep the potential of an electrode across a range of interest and plot the corresponding current response, was performed on solutions of ethyl viologen di-perchlorate (0.05 M), n-methylphthalimide (0.05 M), or PTIO (0.1 M) in acetonitrile with 1 M $NaClO_4$. Voltammetry was performed on both glassy carbon and platinum electrodes and was found to be qualitatively similar to voltammograms previously presented in the literature.[40–42] Voltammetry of all three molecules was then performed in DES and different behavior types were identified. The various electrochemical reactions and voltammetry can be seen in Figure 1. The types of behavior shifts observed when changing the electrolyte from acetonitrile to DES generally fall into one of three categories: 1) no change (Figure 1 "Ethyl Viologen") 2) a shift in the redox potential, but without adverse effects on reversibility (Figure 1 "PTIO"), or 3) a shift to highly irreversible behavior Figure 1 "n-methhylphthalimide). Ethyl viologen and the PTIO positive reaction ($PTIO \rightarrow PTIO^+ \rightarrow PTIO$) show no change in reaction potential or peak current while the PTIO negative reaction ($PTIO \rightarrow PTIO^- \rightarrow PTIO$) appears reversible but undergoes a significant potential shift to more positive potentials. This can be seen in figure 1, indicated by the bar showing distance between the peak-to-peak midpoint for each reaction. Finally, the n-methhylphthalimide compound shows a +1V potential shift in the peak potential of the re-oxidation from the anion form back to the neutral molecule, relative to the peak potential for the reduction reaction, i.e., a shift to highly irreversible behavior. The reduction and oxidation peaks for each reaction are indicated with black arrows. We see that in the acetonitrile electrolyte both redox peaks exist with a very small separation. In the DES electrolyte, no oxidation peak is observed at the expected potentials, but a new oxidation peak is observed at much more positive potentials.

To understand the change in behavior from acetonitrile electrolyte to ChCl:EG, an experiment was devised in which voltammetry was taken in acetonitrile for each of the three species with various additions of the hydrogen bond donor. EG was used in place of the complete DES (ChCl:EG) due to the insolubility of choline chloride in acetonitrile. Remaining in an acetonitrile electrolyte while introducing the presence of a hydrogen bond donor eliminates the difficulty of trying to compare different reference potentials when switching from one solvent to another. This type of analysis can be used to quantify potential shifts rather than make qualitative statements about voltammetry in dissimilar systems. With these samples created at EG to redox organic molar ratios of 0:1, 1:10, 1:1 and 10:1, we also used FTIR to monitor the formation of hydrogen bonds by looking for shifts to lower wave number in the stretching frequencies of known functional groups as the hydrogen bond donor is added and to correlate the presence of any new hydrogen bonds to changes in electrochemical behavior.[43,44]

FTIR-ATR Peak Shift Analysis

FTIR-ATR was performed on neutral PTIO in acetonitrile electrolyte with molar ratios of 0:1, 1:10, 1:1, and 10:1 EG to PTIO, respectively and can be seen in Figure 2. Literature reports that pure EG does not have any strong peaks that overlap in the region we examine.[45] This is confirmed by the lack of additional peaks when EG is added to the pure acetonitrile sample in these regions. The majority of the FTIR peaks associated with PTIO remained unshifted and were subsequently used to normalize spectra to each other. However, the peak associated with the nitroxide radical stretching frequency (identified in the literature as 1218 cm^{-1})[40] had a small red shift that increased with increasing EG concentration. This implies that even the uncharged radical forms weak hydrogen bonds with the electrolyte at the redox active functional group. FTIR-ATR was also performed on N-methylphthalimide in acetonitrile, and no shift was observed in the carbonyl stretching frequency (1710 cm^{-1}) suggesting that no hydrogen bonds are formed with the redox active functional group in this case. The N-methylphthalimide spectra do show a small shift to lower wave number associated with a C-N stretching frequency (1410 cm^{-1}). These results can be seen in Figure 3.

To determine the change in hydrogen bonding as a molecule is reduced, and thus its electron density at the redox active functional group is increased, N-methylphthalimide in acetonitrile was charged in a flow cell with PTIO→$PTIO^+$ as the positive reaction (as described above) at a constant potential of 2.5V. The charged negative electrolyte, now concentrated in the phthalimide anion, was divided into two samples. One was dosed with EG to create a 10:1 molar ratio of EG to phthalimide and the other was left unaltered. FTIR-ATR was performed on the charged electrolyte with and without the ES addition. It was observed that a shift to lower wave number does occur in both the newly observed C-O stretching frequency (~1100 cm^{-1}) and the formerly unshifted carbonyl stretching frequency (1710 cm^{-1}) which can be seen in Figure 3. This suggests that the anion group is now forming a hydrogen bond that did not exist in the uncharged, neutral molecule and that a resonance effect may be sharing the bond between both the conjugated oxygen containing functional groups.

Electrochemical Behavior in Acetonitrile with EG Additions

The voltammetry recorded in acetonitrile with additions of EG tells a similar story. Results of a similar experiment were previously reported for PTIO and can be seen in Sinclair et. al. [25] Those results show that the shift in the peak potentials of both the oxidation and reduction of the negative reaction of PTIO are related to the concentration of EG with a larger potential shift as the EG concentration was increased. No shift was observed in the positive reaction of PTIO (neutral to cation). This is consistent with both the neutral and anion forms forming hydrogen bonds that shift the potential of their respective reactions more positive while the cation does not form hydrogen bonds with EG and does not have its reaction potential affected. Similarly, the ethyl viologen voltammetry, seen in Figure 4, does not change with EG addition, suggesting it does not form a hydrogen bond in either the radical or cation form that would affect its behavior. In the case of n-methylphthalimide, it was found that any addition of EG (even 5 mmol) to acetonitrile immediately shifts the potential of the oxidation peak of n-methylphthalimide suggesting a possible surface adsorption of EG type effect the causes the environment near the electrode to always form hydrogen bonds. Future work is needed to fully understand this phenomenon at such low concentrations.

Polarity and Electrostatic Potential Maps

To gain a better understanding on the mechanism behind the voltammetry differences reported throughout this work for redox species solvated in either ethaline or acetonitrile, we examined the electrostatic potential (ESP) maps of these molecules. Because the previous sections demonstrated that EG alone induces the observed potential shift, the impact of choline chloride (the second component of ethaline) is ignored. The use of ESP maps is a computationally inexpensive framework that qualitatively probes the polarity of molecules at different functional groups and their likelihood of establishing intermolecular interactions.[46,47] The ESPs of each molecule of interest were computed and mapped on the 0.002 a.u density isosurface. These results, obtained using DFT at the B3LYP-D3/def2-TZVPD level of theory, are depicted in Figure 5. Note that a density isovalue of 0.002 a.u. is generally considered an accurate representation of the van der Waals size and shape of molecules, hence being suitable to study intermolecular interactions.[48,49]

Figure 5 confirms that EG possesses both negative and positive ESP surfaces at its hydroxyl functional group sites, thus behaving both as a hydrogen bond donor and acceptor. On the other hand, acetonitrile is an aprotic solvent with a clear negative electrostatic potential at its nitrile functional group but only a faint positive ESP surface at its methyl group. As such, while both solvents will interact favorably with positive ESP surfaces (e.g., hydrogen bond donor sites and positively charged ions), EG possesses the additional ability to establish strong interactions with negative ESP surfaces (e.g., hydrogen bond acceptor sites and negatively charged ions); acetonitrile will generally not interact with negative ESP surfaces.

Focusing on the redox molecules studied in this work, Figure 5 reveals that the neutral forms of PTIO and N-methylphthalimide contain only neutral and negative ESP surfaces, with the latter becoming much more negatively charged in their reduced (negatively charged) forms. As such, these redox molecules, particularly their reduced (anionic) forms, are expected to interact more favorably with EG than with acetonitrile. Furthermore, the hydrogen bond donor sites of EG are expected to interact with the most negatively charged surfaces of PTIO and N-methylphthalimide, which are located on top of their redox-able functional groups. In turn, this strong interaction hinders the necessary electron transfer during a redox reaction, leading to the voltammetry potential shifts observed and reported in the previous sections for the re-oxidation of methylphthalimide and the PTIO negative reaction (PTIO →PTIO$^-$ →PTIO).

To validate the usefulness of the ESP map framework and the accuracy of its qualitative predictions regarding solvent-solute interaction energies discussed above, ESP maps were explicitly calculated using DFT at the B3LYP-D3/def2-TZVPD level of theory, as described in the Methods section. The ESP maps were used as guides to select the initial geometries of the dimers. That is, the molecules were packed such that their main contact occurred between the most negative ESP of the redox molecule and the most positive ESP of the solvent. These results, which are in full agreement with the FTIR results reported in the previous sections, are reported in Figure 6, confirming that the interactions with EG are, indeed, stronger than those with acetonitrile, particularly for the reduced forms of the redox molecules. This type of analysis is introduced and briefly discussed at this point only to validate the qualitative approach of the ESP map framework and will be revisited in the last section of this work to build a semi-empirical correlation.

In contrast with the negative and neutral forms of N-methylphthalimide and PTIO, Figure 5 reveals that the oxidized forms of PTIO and ethyl viologen display only positive electrostatic potentials (to be expected given their positive charges), while the neutral form of ethyl viologen is mostly apolar, with little electrostatic potential beyond that of its aromatic π orbitals. As such, the interaction strength between these species and acetonitrile or EG are similar, which is in line with the absence of changes in reaction potential or peak current for the reduction/oxidation of ethyl viologen and the positive reaction of PTIO (PTIO →PTIO$^+$ →PTIO) reported above.

Molecular Design and Addition of Electron Withdrawing Functional Groups

Despite their qualitative nature, the results shown in Figure 6 suggest that reducing the electrostatic potential of hydrogen-bond-capable redox functional groups should decrease the interaction strength between those sites and the solvent which, in turn, should mitigate or even eliminate voltammetry potential shifts and irreversible reduction/oxidation cycles. This is particularly relevant when dissolving redox molecules in DESs, as these solvents are typically mixtures of strong HBAs and HBDs and, thus, can establish strong hydrogen bonds with solutes. These design considerations are vital in enabling the use of neutral/anion redox couples in which only the anion form creates a hydrogen bond causing apparent extreme irreversibility. To test this hypothesis, the voltammetry of fluorenone was compared to that of the commercially available but less soluble, di-nitro fluorenone. Fluorenone is known to undergo two reduction reactions in acetonitrile but is also reversible in other electrolyte systems.[50–52] Similarly to N-methylphthalimide, the molecule reduces from a neutral species to an anion but fluorenone can additionally be reduced to a di-anion. For the purposes of this study only the first reduction was investigated. Nitro groups are an electron withdrawing group which have been reported to also shift reaction potentials positive but in a reversible manner.[53,54] The electrostatic potential maps of these molecules are depicted in Figure 7.

Figure 7 reveals that fluorenone possesses an almost neutral molecular surface except for its carbonyl functional group site, where it displays a highly negative electrostatic potential, akin to that observed for N-methylphthalimide (Figure 5d). However, upon functionalization with electron withdrawing agents (nitro groups), the intensity of this negative ESP is greatly reduced. In fact, Figure 7b shows that this electron withdrawing effect leads to the appearance of a positive ESP surface that spreads through the aromatic hydrogens of the molecule. The electron withdrawing effect of the nitro groups also produces a remarkable effect in the reduced forms of these redox molecules, with the negative ESP at the carbonyl site of di-nitrofluorenone being drastically lower than that of fluorenone.

Given the polarity differences between fluorenone and di-nitrofluorenone discussed above, the former is anticipated to establish stronger hydrogen bonding with EG than the latter. Of course, both molecules are still expected to interact less favorably with acetonitrile. To confirm these predictions, solvent-solute interaction energies were again computed in the same fashion as the calculations performed in the previous section (DFT at the B3LYP-D3/def2-TZVPD level of theory with molecules being packed such that their main contact occurs between the most negative ESP of the redox molecule and the most positive ESP of the solvent). These results are listed in Figure 8.

The interaction energies reported in Figure 8 confirm that i) EG interacts more favorably with the redox molecules than acetonitrile and ii) the addition of electron withdrawing groups to fluorenone greatly reduces its ability to hydrogen bond with the solvent. More precisely, while the energy difference between the neutral dimers and EG is small (a nearly negligible reduction of 1.4 kJ/mol from fluorenone to di-nitrofluorenone), the energy difference for the anions is remarkable (28.7 kJ/mol).

Voltammetry for these two molecules can be seen in Figure 9. While fluorenone shows an even larger peak separation than N-methylphthalimide (1.5 V), the addition of the nitro groups causes a slight positive shift of the reaction potential but more importantly causes the reaction to now be reversible as predicted by our hypothesis. This demonstrates that reducing the strength of the hydrogen bond interaction at the redox active site is crucial for enabling the reversibility of many redox organic molecules in DES.

Correlating Interaction Energies with Voltammetry Potential

Having demonstrated that certain electron withdrawing groups can modify redox organic behavior in DES for more desirable traits, it is crucial to accurately predict how any such modifications can affect a wide variety of redox molecules. Such a model is important as it helps avoid costly trial and error synthesis.

So far, electrostatic potential maps and dimer interaction energies were used as tools to reconcile the voltammetry potential shifts of different redox molecules in acetonitrile or EG with the intermolecular interaction strengths in these systems. Of course, these methodologies are crude approximations of the highly complex solvation environment of redox molecules in deep eutectic solvents, particularly ethaline. However, despite their simplistic nature, the guidelines developed in this work succeeded in the rational functionalization of a known redox molecule (fluorenone) to prevent its irreversible reduction in ethaline. As such, and to both underpin the results reported throughout this work and reinforce the importance of studying and understanding solvent-solute interactions in DES-mediated redox reactions, the dimer interaction energies reported in Figures 7 and 9 were complemented with those for the remaining redox molecules whose oxidation was studied in this work and correlated against their voltammetry potential from acetonitrile to ethaline. This semi-empirical correlation is depicted in Figure 10. Although the number of data points is small, there is clearly a trend between voltammetry potential shifts and the energy difference between EG-neutral and EG-reduced dimer pairs, which can be used in future work to design new solvent-redox molecule systems.

Conclusions

We have shown through electrochemical, spectroscopic, and molecular modeling techniques that a correlation exists between the redox potential shift of redox organic molecules and their hydrogen bonding behavior in deep eutectic solvent electrolytes. We have shown that this behavior is a function of the electron density near the redox active functional group and can change with oxidation state of the molecule. An electrochemical reduction of the molecule increases local electron density which can increase the strength of, or create a wholly new hydrogen bond to, the redox active site. The presence of these newly formed hydrogen bond has been confirmed through FTIR analysis. This bond now interferes with the redox behavior of the molecule causing a significant positive shift in its oxidation potential. Molecular modeling was used to characterize the strength of these bonds based on the interaction energies of the redox molecule at various oxidation states. The characterization of these hydrogen bond interactions paints the following picture: when a bond is made to a redox functional group, and that bond is above a certain minimum hydrogen bonding energy, there is a positive shift in potential that can be correlated to the strength of the hydrogen bond. Using this correlation to guide intelligent redox molecule design, we show that functionalizing a redox molecule in such a way that lowers the electron density around the redox active functional group lowers the strength of the hydrogen bonding interaction. This prevents the hydrogen bond from interfering with the redox reaction, leading to much greater reversibility in the functionalized molecule than in the base molecule. While further work may be necessary to more accurately predict shifts in redox potential related to hydrogen bonding, this works provides crucial guidance to the design of redox active organic molecules for use in hydrogen bonding electrolytes like deep eutectic solvents.

Acknowledgements

This work was supported as part of the Breakthrough Electrolytes for Energy Storage (BEES), an Energy Frontier Research Center funded by the U.S. Department of Energy, Office of Science, Basic Energy Sciences under Award # DE-SC0019409. This work was also supported within the scope of the project CICECO-Aveiro Institute of Materials, UIDB/50011/2020 (DOI 10.54499/UIDB/50011/2020), UIDP/50011/2020 (DOI 10.54499/UIDP/50011/2020) & LA/P/0006/2020 (DOI 10.54499/LA/P/0006/2020), financed by national funds through the FCT/MCTES (PIDDAC). The authors would like to thank the Center for Research Computing (CRC) at the University of Notre Dame for providing computational resources. The authors have no conflict of interest to declare with any of the work presented here.

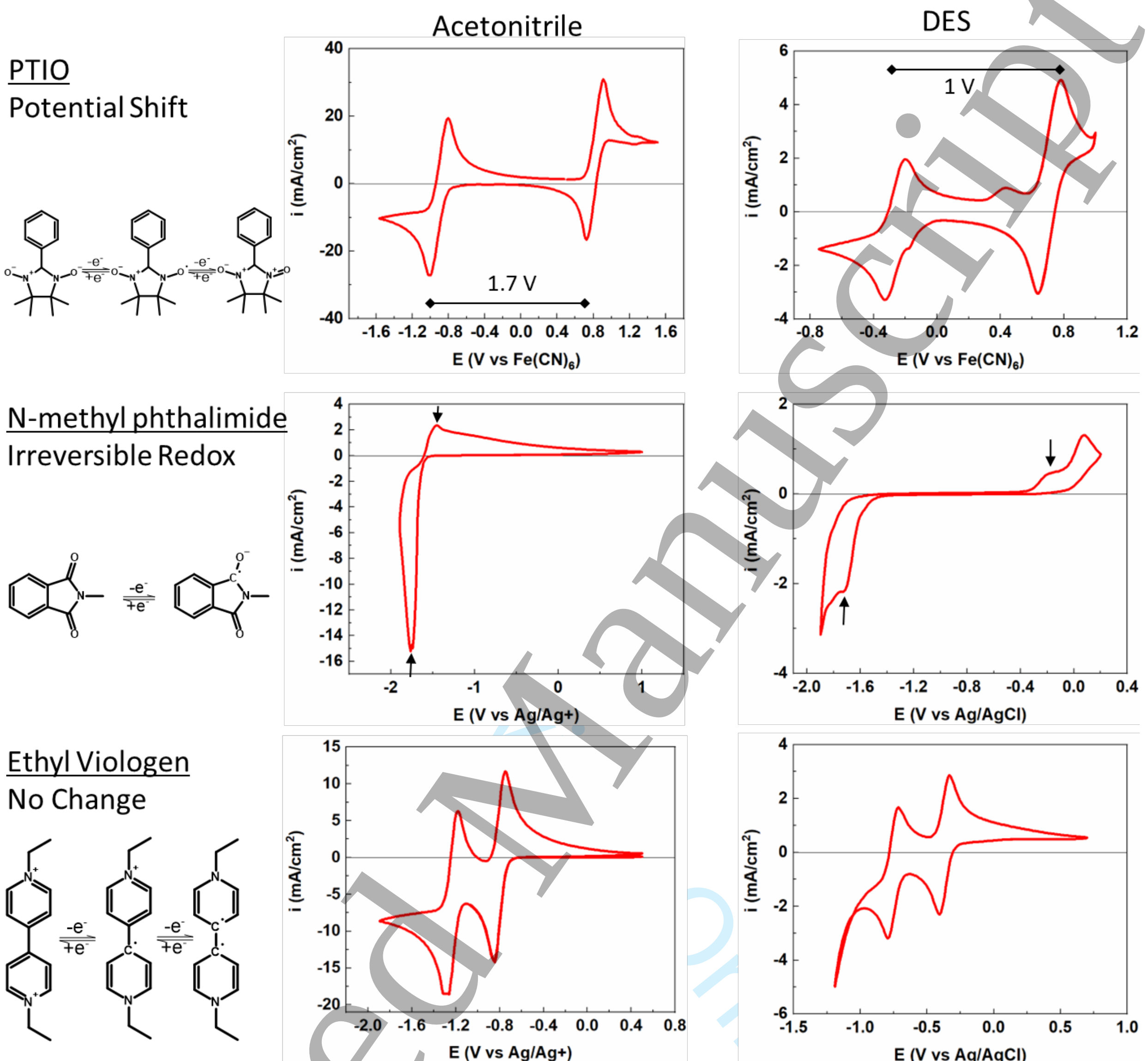

Figure 1. Reactions and voltammetry for PTIO, N-methylphthalimide and ethyl viologen in both acetonitrile and a 1:4 molar ratio mixture of choline chloride and EG, respectively, exhibit three distinct types of behavior. PTIO exhibits a 700 mV shift in the $E_{1/2}$ of the negative reaction when transitioning to DES. N-methylphthalimide shows 1 V increase in peak separation while ethyl viologen remains unaffected.

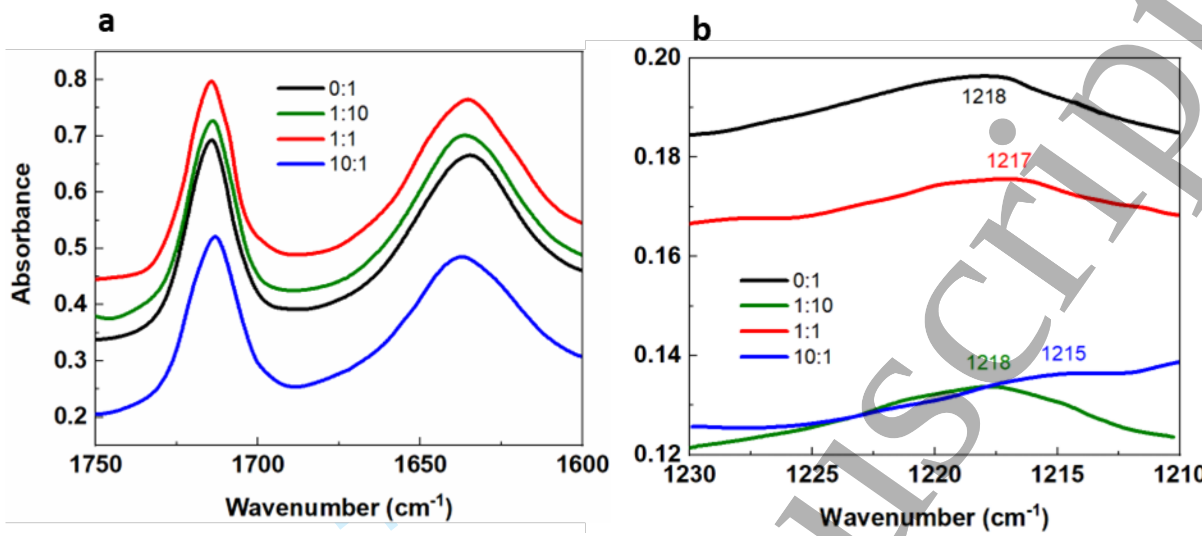

Figure 2. Uncharged N-methylphthalimide (a) and PTIO (b) FTIR-ATR spectra of the respective molecule dissolved in acetonitrile electrolyte as a function of EG to redox organic molar ratio shows no change in the stretching frequency associated with the redox active carbonyl group in N-methylphthalimide and a small red shift in the stretching frequency of the nitroxide radical as EG concentration is increased.

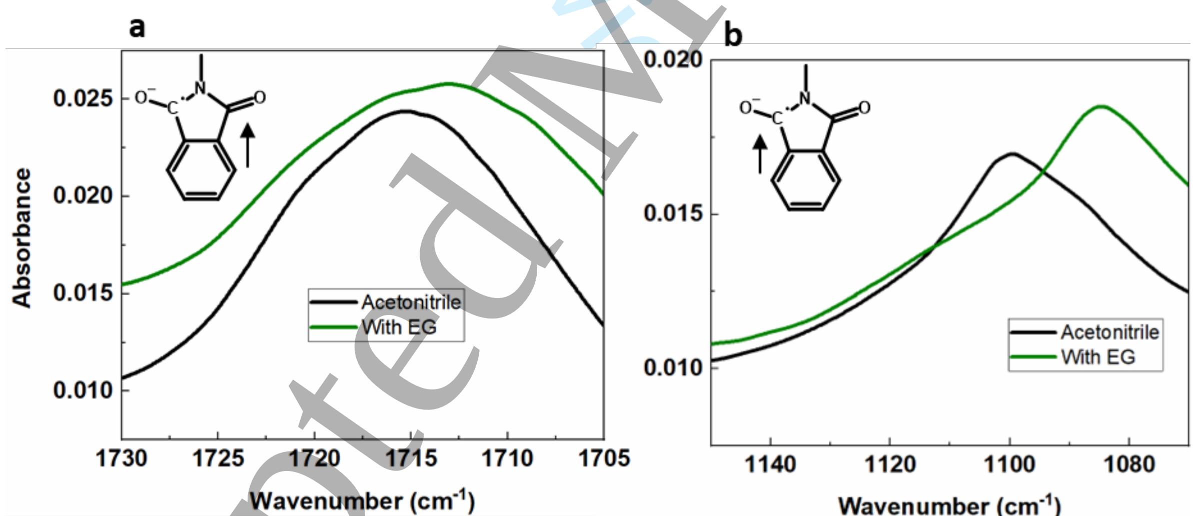

Figure 3. Charged N-methylphthalimide acetonitrile electrolyte with and without a 10:1 EG:phthalimide molar ratio addition of EG shows a red shift in both the C-O stretching peak (left) and a lesser shift in the carbonyl stretching peak (right).

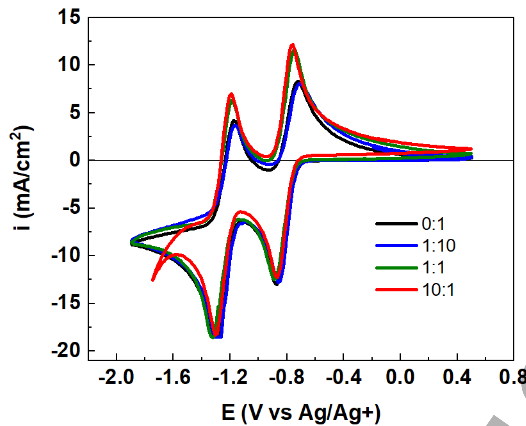

Figure 4. Voltammetry of ethyl viologen in acetonitrile electrolyte with increasing concentrations of EG shows now change peak potential and even a slight increase in peak potential as EG is added.

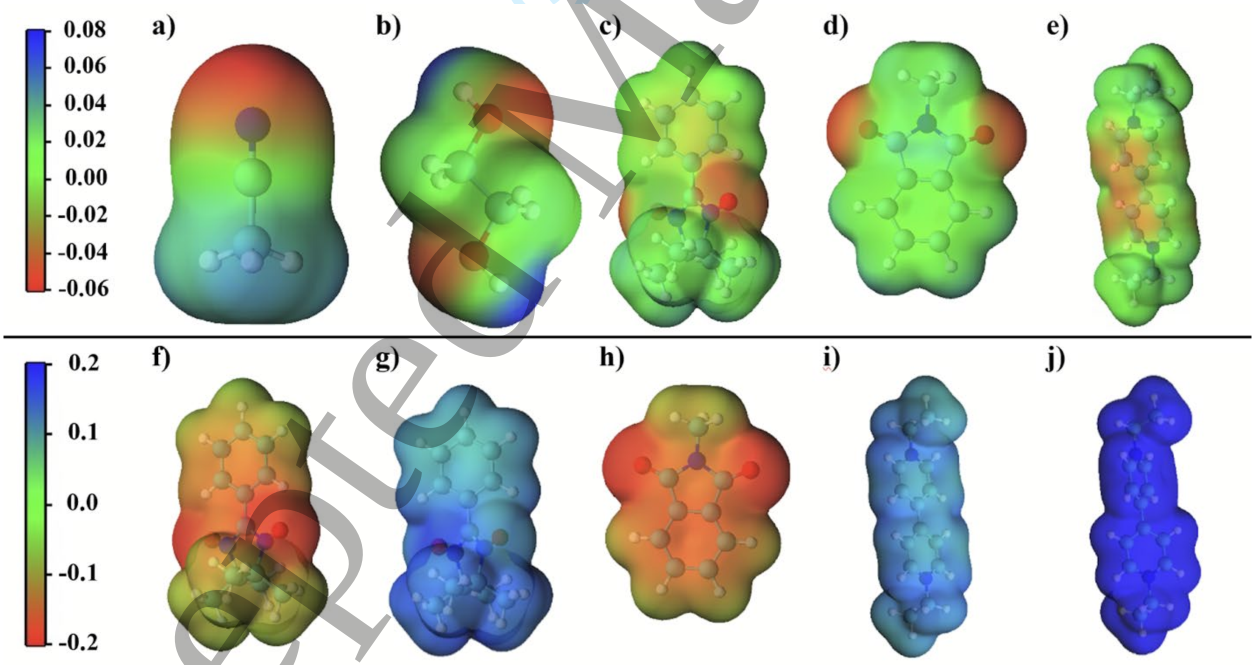

Figure 5. Top panel: electrostatic potential mapped and color-coded on the density isosurface (isovalue of 0.002 a.u.) of acetonitrile (a), EG (b), and the neutral forms of PTIO (c), N-methylphthalimide (d), and ethyl viologen (e). Bottom panel: electrostatic potential mapped and color-coded on the density isosurface (isovalue of 0.002 a.u.) of the reduced (f) and oxidized (g) forms of PTIO, the reduced form of N-methylphthalimide (h), and the oxidized form (i) and double

oxidized (j) forms of ethyl viologen. All calculations were performed at the B3LYP-D3/def2-TZVPD level of theory. Color bars represent the electrostatic potential in atomic units.

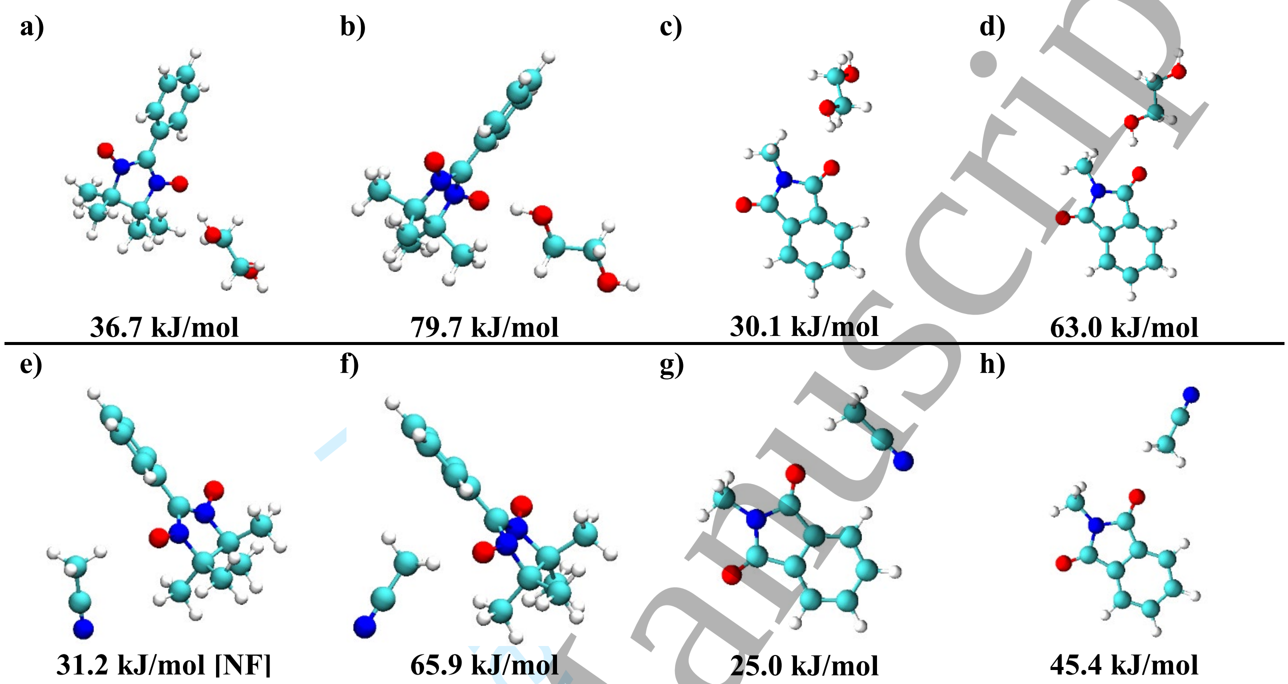

Figure 6. Interaction energies between EG (top panel) or acetonitrile (bottom panel) and the neutral (a and e) and reduced (b and f) forms of PTIO or the neutral (c and g) and reduced (d and h) forms of N-methylphthalimide. All calculations were performed at the B3LYP-D3/def2-TZVPD level of theory.

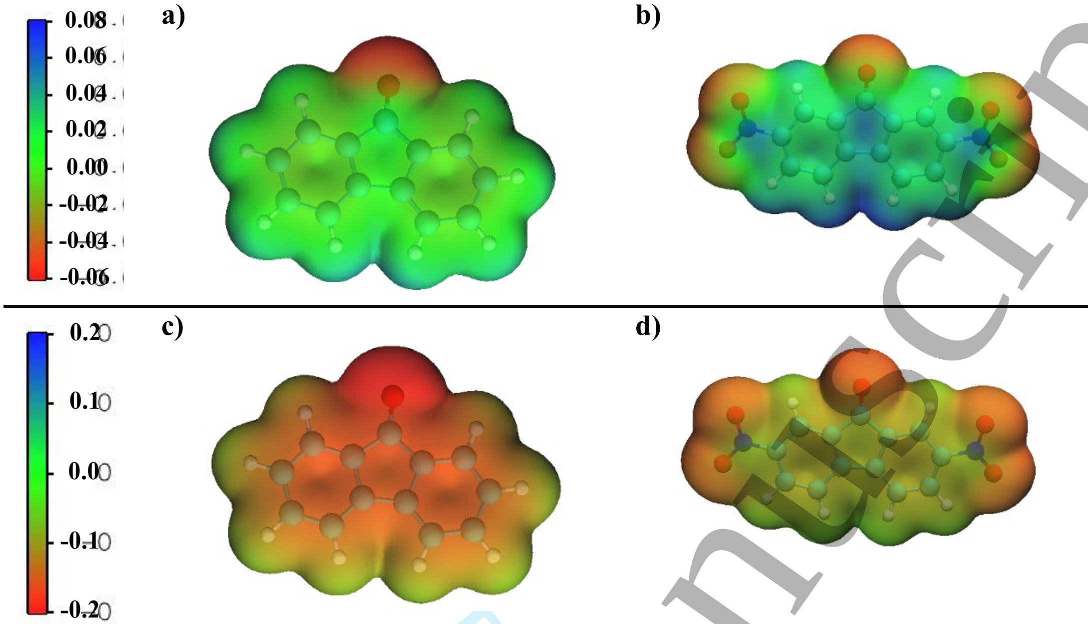

Figure 7. Top panel: electrostatic potential mapped and color-coded on the density isosurface (isovalue of 0.002 a.u.) of fluorenone (a) and di-nitro fluorenone (b). Bottom panel: electrostatic potential mapped and color-coded on the density isosurface (isovalue of 0.002 a.u.) of the reduced forms of fluorenone (c) and di-nitrofluorenone (d). All calculations were performed at the B3LYP-D3/def2-TZVPD level of theory. Color bars represent the electrostatic potential in atomic units.

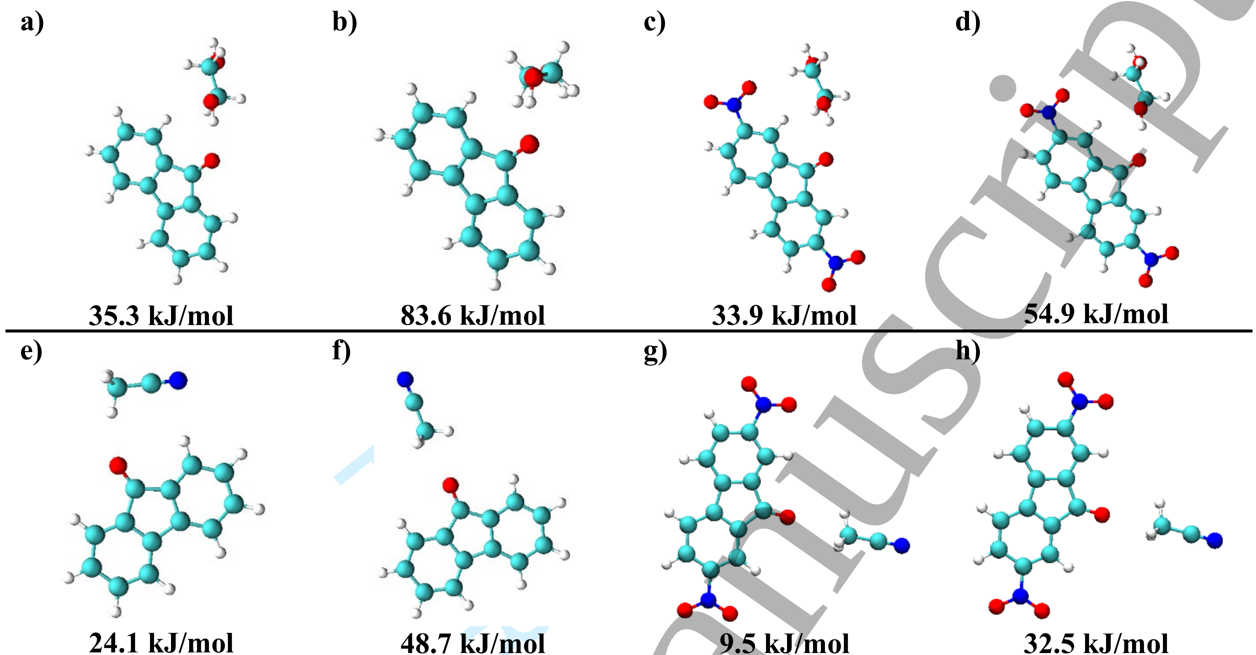

Figure 8. Interaction energies between EG (top panel) or acetonitrile (bottom panel) and the neutral (a and e) and reduced (b and f) forms of fluorenone or the neutral (c and g) and reduced (d and h) forms of di-nitrofluorenone. All calculations were performed at the B3LYP-D3/def2-TZVPD level of theory.

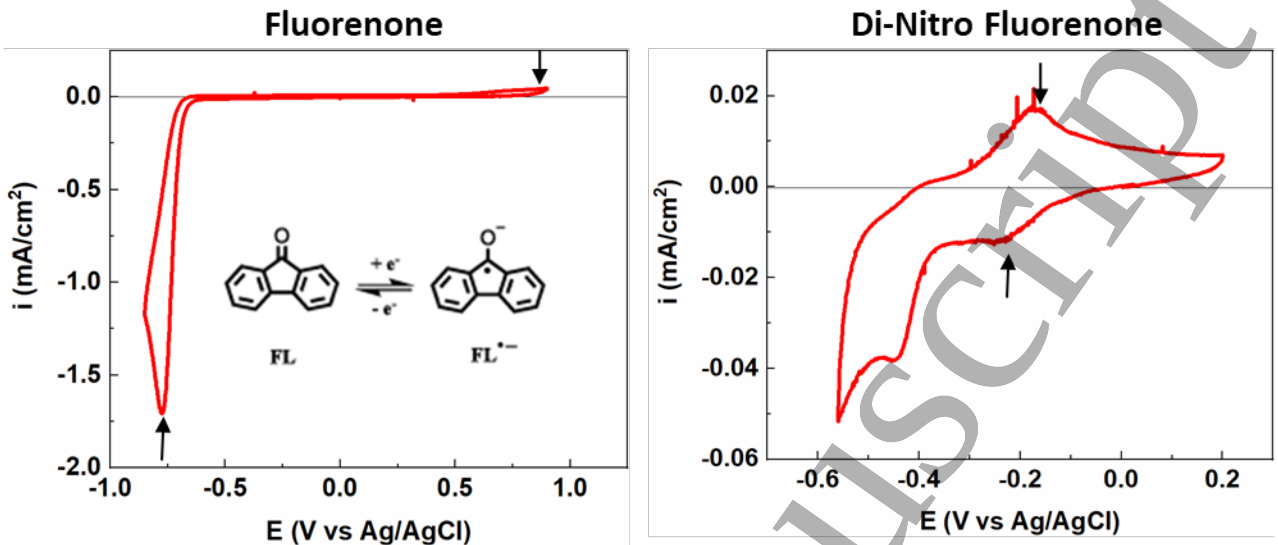

Figure 9. Voltammetry of fluorenone and di-nitro fluorenone shows that a 1.5 V positive shift exists in the re-oxidation of the fluorenone anion. The addition of electron withdrawing nitro groups shifts the potential of both the first and second reduction more positive but enables the reversible oxidation of the anion back to the neutral species.

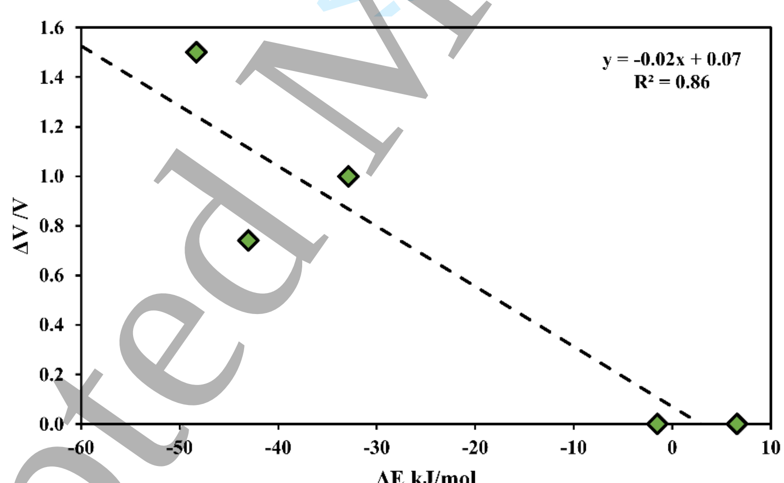

Figure 10. Voltammetry potential shifts from acetonitrile to ethaline during the oxidation of the redox species studied in this work as a function of the energy difference between EG-neutral and EG-reduced dimer pairs. These shifts trend approximately linearly.

References

(1) D'Aprile, P.; Newman, J.; Pinner, D. The New Economics of Energy Storage | McKinsey. *Mckinsey&Company - Sustainability & Resource Productivity* **2016**, 1–9.

(2) St.John, J. Global Energy Storage Markets Will Grow 13-Fold from 2018 to 2024 to Reach 158 Gigawatt-Hours and Billion in Investment, Wood Mackenzie Power & Renewables Reports. *Green Tech Media*. 2019.

(3) Pleßmann, G.; Erdmann, M.; Hlusiak, M.; Breyer, C. Global Energy Storage Demand for a 100% Renewable Electricity Supply. In *Energy Procedia*; Elsevier Ltd, 2014; Vol. 46, pp 22–31. https://doi.org/10.1016/j.egypro.2014.01.154.

(4) Zhang, C.; Zhang, L.; Ding, Y.; Peng, S.; Guo, X.; Zhao, Y.; He, G.; Yu, G. Progress and Prospects of Next-Generation Redox Flow Batteries. *Energy Storage Mater* **2018**, *15*, 324–350. https://doi.org/10.1016/J.ENSM.2018.06.008.

(5) Skyllas-Kazacos, M.; Chakrabarti, M. H.; Hajimolana, S. A.; Mjalli, F. S.; Saleem, M. Progress in Flow Battery Research and Development. *Journal of the Electrochemical Society*. August 2011. https://doi.org/10.1149/1.3599565.

(6) Sun, C. N.; Mench, M. M.; Zawodzinski, T. A. High Performance Redox Flow Batteries: An Analysis of the Upper Performance Limits of Flow Batteries Using Non-Aqueous Solvents. *Electrochim Acta* **2017**, *237*, 199–206. https://doi.org/10.1016/j.electacta.2017.03.132.

(7) Milshtein, J. D.; Darling, R. M.; Drake, J.; Perry, M. L.; Brushett, F. R. The Critical Role of Supporting Electrolyte Selection on Flow Battery Cost. *J Electrochem Soc* **2017**, *164* (14), A3883–A3895. https://doi.org/10.1149/2.1031714jes.

(8) Liu, Q.; Sleightholme, A. E. S.; Shinkle, A. A.; Li, Y.; Thompson, L. T. Non-Aqueous Vanadium Acetylacetonate Electrolyte for Redox Flow Batteries. *Electrochem commun* **2009**, *11* (12), 2312–2315. https://doi.org/10.1016/J.ELECOM.2009.10.006.

(9) Leung, P.; Shah, A. A.; Sanz, L.; Flox, C.; Morante, J. R.; Xu, Q.; Mohamed, M. R.; Ponce de León, C.; Walsh, F. C. Recent Developments in Organic Redox Flow Batteries: A Critical Review. *Journal of Power Sources*. Elsevier B.V. 2017, pp 243–283. https://doi.org/10.1016/j.jpowsour.2017.05.057.

(10) Chen, B.; Mitchell, S.; Sinclair, N.; Wainright, J.; Pentzer, E.; Gurkan, B. Feasibility of TEMPO-Functionalized Imidazolium, Ammonium and Pyridinium Salts as Redox-Active Carriers in Ethaline Deep Eutectic Solvent for Energy Storage. *Mol Syst Des Eng* **2020**, *5* (6), 1147–1157. https://doi.org/10.1039/D0ME00038H.

(11) Aaron, D. S.; Liu, Q.; Tang, Z.; Grim, G. M.; Papandrew, A. B.; Turhan, A.; Zawodzinski, T. A.; Mench, M. M. Dramatic Performance Gains in Vanadium Redox Flow Batteries through Modified Cell Architecture. *J Power Sources* **2011**, *206*, 450–453. https://doi.org/10.1016/j.jpowsour.2011.12.026.

(12) Hansen, B. B.; Spittle, S.; Chen, B.; Poe, D.; Zhang, Y.; Klein, J. M.; Horton, A.; Adhikari, L.; Zelovich, T.; Doherty, B. W.; Gurkan, B.; Maginn, E. J.; Ragauskas, A.; Dadmun, M.; Zawodzinski, T. A.; Baker, G. A.; Tuckerman, M. E.; Savinell, R. F.; Sangoro, J. R. Deep Eutectic Solvents: A Review of Fundamentals and Applications. *Chem Rev* **2021**, *121* (3), 1232–1285. https://doi.org/10.1021/ACS.CHEMREV.0C00385/ASSET/IMAGES/MEDIUM/CR0C00385_0009.GIF.

(13) Abranches, D. O.; Coutinho, J. A. P. Everything You Wanted to Know about Deep Eutectic Solvents but Were Afraid to Be Told. *Annu Rev Chem Biomol Eng* **2023**, *14* (1), 141–163. https://doi.org/10.1146/annurev-chembioeng-101121-085323.

(14) Abbott, A. P.; Capper, G.; McKenzie, K. J.; Ryder, K. S. Electrodeposition of Zinc–Tin Alloys from Deep Eutectic Solvents Based on Choline Chloride. *Journal of Electroanalytical Chemistry* **2007**, *599* (2), 288–294. https://doi.org/https://doi.org/10.1016/j.jelechem.2006.04.024.

(15) Abbott, A. P.; Capper, G.; Swain, B. G.; Wheeler, D. A. Electropolishing of Stainless Steel in an Ionic Liquid. *Transactions of the IMF* **2005**, *83* (1), 51–53. https://doi.org/10.1179/002029605X17657.

(16) Liao, H.-G.; Jiang, Y.-X.; Zhou, Z.-Y.; Chen, S.-P.; Sun, S.-G. Shape-Controlled Synthesis of Gold Nanoparticles in Deep Eutectic Solvents for Studies of Structure–Functionality Relationships in Electrocatalysis. *Angewandte Chemie International Edition* **2008**, *47* (47), 9100–9103. https://doi.org/https://doi.org/10.1002/anie.200803202.

(17) Abbott, A. P.; Boothby, D.; Capper, G.; Davies, D. L.; Rasheed, R. K. Deep Eutectic Solvents Formed between Choline Chloride and Carboxylic Acids: Versatile Alternatives to Ionic Liquids. *J Am Chem Soc* **2004**, *126* (29), 9142–9147. https://doi.org/10.1021/ja048266j.

(18) Abbott, A. P.; Capper, G.; Davies, D. L.; Rasheed, R. K.; Tambyrajah, V. Novel Solvent Properties of Choline Chloride/Urea Mixtures. *Chemical Communications* **2003**, No. 1, 70–71. https://doi.org/10.1039/b210714g.

(19) Wu, S.-H.; Caparanga, A. R.; Leron, R. B.; Li, M.-H. Vapor Pressure of Aqueous Choline Chloride-Based Deep Eutectic Solvents (Ethaline, Glyceline, Maline and Reline) at 30–70°C. *Thermochim Acta* **2012**, *544*, 1–5. https://doi.org/10.1016/j.tca.2012.05.031.

(20) Delgado-Mellado, N.; Larriba, M.; Navarro, P.; Rigual, V.; Ayuso, M.; García, J.; Rodríguez, F. Thermal Stability of Choline Chloride Deep Eutectic Solvents by TGA/FTIR-ATR Analysis. *J Mol Liq* **2018**, *260*, 37–43. https://doi.org/10.1016/j.molliq.2018.03.076.

(21) Chakrabarti, M. H.; Mjalli, F. S.; AlNashef, I. M.; Hashim, Mohd. A.; Hussain, Mohd. A.; Bahadori, L.; Low, C. T. J. Prospects of Applying Ionic Liquids and Deep Eutectic Solvents for Renewable Energy Storage by Means of Redox Flow Batteries. *Renewable and Sustainable Energy Reviews* **2014**, *30*, 254–270. https://doi.org/https://doi.org/10.1016/j.rser.2013.10.004.

(22) Miller, M. A.; Wainright, J. S.; Savinell, R. F. Iron Electrodeposition in a Deep Eutectic Solvent for Flow Batteries. *J Electrochem Soc* **2017**, *164* (4), A796–A803. https://doi.org/10.1149/2.1141704jes.

(23) Lloyd, D.; Vainikka, T.; Kontturi, K. The Development of an All Copper Hybrid Redox Flow Battery Using Deep Eutectic Solvents. *Electrochim Acta* **2013**, *100*, 18–23. https://doi.org/10.1016/J.ELECTACTA.2013.03.130.

(24) Goeltz, J. C.; Matsushima, L. N. Metal-Free Redox Active Deep Eutectic Solvents †. *Chem. Commun* **2017**, *53*, 9983. https://doi.org/10.1039/c7cc04837h.

(25) Sinclair, N. S.; Poe, D.; Savinell, R. F.; Maginn, E. J.; Wainright, J. S. A Nitroxide Containing Organic Molecule in a Deep Eutectic Solvent for Flow Battery Applications. *J Electrochem Soc* **2021**, *168* (2), 20527. https://doi.org/10.1149/1945-7111/abe28a.

(26) Ghahremani, R.; Savinell, R. F.; Gurkan, B. Perspective—Hydrogen Bonded Concentrated Electrolytes for Redox Flow Batteries: Limitations and Prospects. *J Electrochem Soc* **2022**, *169* (3), 30520. https://doi.org/10.1149/1945-7111/ac58c6.

(27) Bezerra, R. C.; Mendes, P. C. D.; Passos, R. R.; Da Silva, J. L. F. Ab Initio Investigation of the Role of Transition-Metal Dopants in the Adsorption Properties of Ethylene Glycol on Doped Pt(100) Surfaces. *Physical Chemistry Chemical Physics* **2020**, *22* (31), 17646–17658. https://doi.org/10.1039/d0cp01403f.

(28) Gilli, G.; Gilli, P. Towards an Unified Hydrogen-Bond Theory. *J Mol Struct* **2000**, *552* (1–3), 1–15. https://doi.org/10.1016/S0022-2860(00)00454-3.

(29) Parthasarathi, R.; Subramanian, V.; Sathyamurthy, N. Hydrogen Bonding without Borders: An Atoms-in-Molecules Perspective. *Journal of Physical Chemistry A* **2006**, *110* (10), 3349–3351. https://doi.org/10.1021/jp060571z.

(30) D'Oria, E.; Novoa, J. J. Cation-Anion Hydrogen Bonds: A New Class of Hydrogen Bonds That Extends Their Strength beyond the Covalent Limit. A Theoretical Characterization. *Journal of Physical Chemistry A* **2011**, *115* (45), 13114–13123. https://doi.org/10.1021/jp205176e.

(31) Tang, T.-H.; Deretey, E.; Knak Jensen, S. J.; Csizmadia, I. G. Hydrogen Bonds: Relation between Lengths and Electron Densities at Bond Critical Points. *The European Physical Journal D - Atomic, Molecular, Optical and Plasma Physics* **2006**, *37* (2), 217–222. https://doi.org/10.1140/epjd/e2005-00317-0.

(32) Zhou, F.; Wang, J.; Zhang, Y.; Wang, Q.; Guo, C.; Wang, F.; Zheng, X.; Zhang, H. Theoretical Studies on the Bond Strength and Electron Density Characteristics in Multiple Hydrogen Bonded Arrays. *J Mol Graph Model* **2019**, *93*, 107439. https://doi.org/https://doi.org/10.1016/j.jmgm.2019.107439.

(33) Gurkan, B.; Squire, H.; Pentzer, E. Metal-Free Deep Eutectic Solvents: Preparation, Physical Properties, and Significance. *J Phys Chem Lett* **2019**, *10* (24), 7956–7964. https://doi.org/10.1021/acs.jpclett.9b01980.

(34) Sinclair, N. S.; Poe, D.; Savinell, R. F.; Maginn, E. J.; Wainright, J. S. A Nitroxide Containing Organic Molecule in a Deep Eutectic Solvent for Flow Battery Applications. *J Electrochem Soc* **2021**, *168* (2), 020527. https://doi.org/10.1149/1945-7111/abe28a.

(35) Ke, X.; Prahl, J. M.; Alexander, J. I. D.; Savinell, R. F. Mathematical Modeling of Electrolyte Flow in a Segment of Flow Channel over Porous Electrode Layered System in Vanadium Flow Battery with Flow Field Design. *Electrochim Acta* **2017**, *223*, 124–134. https://doi.org/10.1016/j.electacta.2016.12.017.

(36) Valiev, M.; Bylaska, E. J.; Govind, N.; Kowalski, K.; Straatsma, T. P.; Van Dam, H. J. J.; Wang, D.; Nieplocha, J.; Apra, E.; Windus, T. L.; De Jong, W. A. NWChem: A Comprehensive and Scalable Open-Source Solution for Large Scale Molecular Simulations. *Comput Phys Commun* **2010**, *181* (9), 1477–1489. https://doi.org/10.1016/J.CPC.2010.04.018.

(37) Aprà, E.; Bylaska, E. J.; De Jong, W. A.; Govind, N.; Kowalski, K.; Straatsma, T. P.; Valiev, M.; Van Dam, H. J. J.; Alexeev, Y.; Anchell, J.; Anisimov, V.; Aquino, F. W.; Atta-Fynn, R.; Autschbach, J.; Bauman, N. P.; Becca, J. C.; Bernholdt, D. E.; Bhaskaran-Nair, K.; Bogatko, S.; Borowski, P.; Boschen, J.; Brabec, J.; Bruner, A.; Cauët, E.; Chen, Y.; Chuev, G. N.; Cramer, C. J.; Daily, J.; Deegan, M. J. O.; Dunning, T. H.; Dupuis, M.; Dyall, K. G.; Fann, G. I.; Fischer, S. A.; Fonari, A.; Früchtl, H.; Gagliardi, L.; Garza, J.; Gawande, N.; Ghosh, S.; Glaesemann, K.; Götz, A. W.; Hammond, J.; Helms, V.; Hermes, E. D.; Hirao, K.; Hirata, S.; Jacquelin, M.; Jensen, L.; Johnson, B. G.; Jónsson, H.; Kendall, R. A.; Klemm, M.; Kobayashi, R.; Konkov, V.; Krishnamoorthy, S.; Krishnan, M.; Lin, Z.; Lins, R. D.; Littlefield, R. J.; Logsdail, A. J.; Lopata, K.; Ma, W.; Marenich, A. V.; Martin Del Campo, J.; Mejia-Rodriguez, D.; Moore, J. E.; Mullin, J. M.; Nakajima, T.; Nascimento, D. R.; Nichols, J. A.; Nichols, P. J.; Nieplocha, J.; Otero-De-La-Roza, A.; Palmer, B.; Panyala, A.; Pirojsirikul, T.; Peng, B.; Peverati, R.; Pittner, J.; Pollack, L.; Richard, R. M.; Sadayappan, P.; Schatz, G. C.; Shelton, W. A.; Silverstein, D. W.; Smith, D. M. A.; Soares, T. A.; Song, D.; Swart, M.; Taylor, H. L.; Thomas, G. S.; Tipparaju, V.; Truhlar, D. G.; Tsemekhman, K.; Van Voorhis, T.; Vázquez-Mayagoitia, A.; Verma, P.; Villa, O.; Vishnu, A.; Vogiatzis, K. D.; Wang, D.; Weare, J. H.; Williamson, M. J.; Windus, T. L.; Woliński, K.; Wong, A. T.; Wu, Q.; Yang, C.; Yu, Q.; Zacharias, M.; Zhang, Z.; Zhao, Y.; Harrison, R. J. NWChem: Past, Present, and Future. *J Chem Phys* **2020**, *152* (18), 184102. https://doi.org/10.1063/5.0004997.

(38) Becke, A. D. Density-functional Thermochemistry. III. The Role of Exact Exchange. *J Chem Phys* **1998**, *98* (7), 5648. https://doi.org/10.1063/1.464913.

(39) Grimme, S.; Antony, J.; Ehrlich, S.; Krieg, H. A Consistent and Accurate Ab Initio Parametrization of Density Functional Dispersion Correction (DFT-D) for the 94 Elements H-Pu. *J Chem Phys* **2010**, *132* (15), 154104. https://doi.org/10.1063/1.3382344.

(40) Duan, W.; Vemuri, R. S.; Milshtein, J. D.; Laramie, S.; Dmello, R. D.; Huang, J.; Zhang, L.; Hu, D.; Vijayakumar, M.; Wang, W.; Liu, J.; Darling, R. M.; Thompson, L.; Smith, K.; Moore, J. S.; Brushett, F. R.; Wei, X. A Symmetric Organic-Based Nonaqueous Redox Flow Battery and Its State of Charge Diagnostics by FTIR. *J Mater Chem A Mater* **2016**, *4* (15), 5448–5456. https://doi.org/10.1039/C6TA01177B.

(41) Li, Z.; Li, S.; Liu, S.; Huang, K.; Fang, D.; Wang, F.; Peng, S. Electrochemical Properties of an All-Organic Redox Flow Battery Using 2,2,6,6-Tetramethyl-1-Piperidinyloxy and N-Methylphthalimide. *Electrochemical and Solid-State Letters* **2011**, *14* (12), A171. https://doi.org/10.1149/2.012112ESL/XML.

(42) Cook, S. K.; Horrocks, B. R. Heterogeneous Electron-Transfer Rates for the Reduction of Viologen Derivatives at Platinum and Bismuth Electrodes in Acetonitrile. *ChemElectroChem* **2017**, *4* (2), 320–331. https://doi.org/10.1002/celc.201600536.

(43) Allen, G.; Colclough, R. O. Hydrogen Bonding of the Thiol Group in Phosphinodithioic Acids. *Journal of the Chemical Society (Resumed)* **1957**, No. 0, 3912–3915. https://doi.org/10.1039/jr9570003912.

(44) Mishra, K. K.; Borish, K.; Singh, G.; Panwaria, P.; Metya, S.; Madhusudhan, M. S.; Das, A. Observation of an Unusually Large IR Red-Shift in an Unconventional S–H···S Hydrogen-Bond. *J Phys Chem Lett* **2021**, *12* (4), 1228–1235. https://doi.org/10.1021/acs.jpclett.0c03183.

(45) Smith, A. L. The Coblentz Society Desk Book of Infrared Spectra, Coblnetz Soc. *Kirkw. MO* **1982**.

(46) Suresh, C. H.; Remya, G. S.; Anjalikrishna, P. K. Molecular Electrostatic Potential Analysis: A Powerful Tool to Interpret and Predict Chemical Reactivity. *WIREs Computational Molecular Science* **2022**, *12* (5), e1601. https://doi.org/https://doi.org/10.1002/wcms.1601.

(47) Scrocco, E.; Tomasi, J. The Electrostatic Molecular Potential as a Tool for the Interpretation of Molecular Properties. In *New Concepts II*; Springer Berlin Heidelberg: Berlin, Heidelberg, 1973; pp 95–170.

(48) Bader, R. F. W.; Henneker, W. H.; Cade, P. E. Molecular Charge Distributions and Chemical Binding. *J Chem Phys* **2004**, *46* (9), 3341. https://doi.org/10.1063/1.1841222.

(49) Purvis, G. D. On the Use of Isovalued Surfaces to Determine Molecule Shape and Reaction Pathways. *Journal of Computer-Aided Molecular Design 1991 5:1* **1991**, *5* (1), 55–80. https://doi.org/10.1007/BF00173470.

(50) Kwon, G.; Lee, K.; Lee, M. H.; Lee, B.; Lee, S.; Jung, S. K.; Ku, K.; Kim, J.; Park, S. Y.; Kwon, J. E.; Kang, K. Bio-Inspired Molecular Redesign of a Multi-Redox Catholyte for High-Energy Non-Aqueous Organic Redox Flow Batteries. *Chem* **2019**, *5* (10), 2642–2656. https://doi.org/10.1016/j.chempr.2019.07.006.

(51) Feng, R.; Zhang, X.; Murugesan, V.; Hollas, A.; Chen, Y.; Shao, Y.; Walter, E.; Wellala, N. P. N.; Yan, L.; Rosso, K. M.; Wang, W. Reversible Ketone Hydrogenation and Dehydrogenation for Aqueous Organic Redox Flow Batteries. *Science (1979)* **2021**, *372* (6544), 836–840. https://doi.org/10.1126/science.abd9795.

(52) Rodriguez, J.; Niemet, C.; Pozzo, L. D. Fluorenone Based Anolyte for an Aqueous Organic Redox-Flow Battery. *ECS Trans* **2019**, *89* (1), 49–59. https://doi.org/10.1149/08901.0049ecst.

(53) Pelzer, K. M.; Cheng, L.; Curtiss, L. A. Effects of Functional Groups in Redox-Active Organic Molecules: A High-Throughput Screening Approach. *The Journal of Physical Chemistry C* **2017**, *121* (1), 237–245. https://doi.org/10.1021/acs.jpcc.6b11473.

(54) Yan, Y.; Robinson, S. G.; Vaid, T. P.; Sigman, M. S.; Sanford, M. S. Simultaneously Enhancing the Redox Potential and Stability of Multi-Redox Organic Catholytes by Incorporating Cyclopropenium Substituents. *J Am Chem Soc* **2021**, *143* (33), 13450–13459. https://doi.org/10.1021/jacs.1c07237.